

Measurement of the Depth of Maximum of Extensive Air Showers above 10^{18} eV

(The Pierre Auger Collaboration)

J. Abraham,¹ P. Abreu,² M. Aglietta,³ E.J. Ahn,⁴ D. Allard,⁵ I. Allekotte,⁶ J. Allen,⁷ J. Alvarez-Muñiz,⁸ M. Ambrosio,⁹ L. Anchordoqui,¹⁰ S. Andringa,² T. Antičić,¹¹ A. Anzalone,¹² C. Aramo,⁹ E. Arganda,¹³ K. Arisaka,¹⁴ F. Arqueros,¹³ H. Asorey,⁶ P. Assis,² J. Aublin,¹⁵ M. Ave,^{16,17} G. Avila,¹⁸ T. Bäcker,¹⁹ D. Badagnani,²⁰ M. Balzer,²¹ K.B. Barber,²² A.F. Barbosa,²³ S.L.C. Barroso,²⁴ B. Baughman,²⁵ P. Bauleo,²⁶ J.J. Beatty,²⁵ B.R. Becker,²⁷ K.H. Becker,²⁸ A. Bellétoile,²⁹ J.A. Bellido,²² S. BenZvi,³⁰ C. Berat,²⁹ T. Bergmann,²¹ X. Bertou,⁶ P.L. Biermann,³¹ P. Billoir,¹⁵ O. Blanch-Bigas,¹⁵ F. Blanco,¹³ M. Blanco,³² C. Bleve,³³ H. Blümer,^{34,16} M. Boháčová,^{17,35} D. Boncioli,³⁶ C. Bonifazi,¹⁵ R. Bonino,³ N. Borodai,³⁷ J. Brack,²⁶ P. Brogueira,² W.C. Brown,³⁸ R. Bruijn,³⁹ P. Buchholz,¹⁹ A. Bueno,⁴⁰ R.E. Burton,⁴¹ N.G. Busca,⁵ K.S. Caballero-Mora,³⁴ L. Caramete,³¹ R. Caruso,⁴² A. Castellina,³ O. Catalano,¹² G. Cataldi,³³ L. Cazon,^{2,17} R. Cester,⁴³ J. Chauvin,²⁹ A. Chiavassa,³ J.A. Chinellato,⁴⁴ A. Chou,^{4,7} J. Chudoba,³⁵ R.W. Clay,²² E. Colombo,⁴⁵ M.R. Coluccia,³³ R. Conceição,² F. Contreras,⁴⁶ H. Cook,³⁹ M.J. Cooper,²² J. Coppens,^{47,48} A. Cordier,⁴⁹ U. Cotti,⁵⁰ S. Coutu,⁵¹ C.E. Covault,⁴¹ A. Creusot,⁵² A. Criss,⁵¹ J. Cronin,¹⁷ A. Curutiu,³¹ S. Dagoret-Campagne,⁴⁹ R. Dallier,⁵³ K. Daumiller,¹⁶ B.R. Dawson,²² R.M. de Almeida,⁴⁴ M. De Domenico,⁴² C. De Donato,^{54,55} S.J. de Jong,⁴⁷ G. De La Vega,¹ W.J.M. de Mello Junior,⁴⁴ J.R.T. de Mello Neto,⁵⁶ I. De Mitri,³³ V. de Souza,⁵⁷ K.D. de Vries,⁵⁸ G. Decerprit,⁵ L. del Peral,³² O. Deligny,⁵⁹ A. Della Selva,⁹ C. Delle Fratte,³⁶ H. Dembinski,⁶⁰ C. Di Giulio,³⁶ J.C. Diaz,⁶¹ M.L. Díaz Castro,⁶² P.N. Diep,⁶³ C. Dobrigkeit,⁴⁴ J.C. D'Olivo,⁵⁴ P.N. Dong,^{63,59} A. Dorofeev,²⁶ J.C. dos Anjos,²³ M.T. Dova,²⁰ D. D'Urso,⁹ I. Dutan,³¹ M.A. DuVernois,⁶⁴ J. Ebr,³⁵ R. Engel,¹⁶ M. Erdmann,⁶⁰ C.O. Escobar,⁴⁴ A. Etchegoyen,⁴⁵ P. Facal San Luis,^{17,8} H. Falcke,^{47,65} G. Farrar,⁷ A.C. Fauth,⁴⁴ N. Fazzini,⁴ A. Ferrero,⁴⁵ B. Fick,⁶¹ A. Filevich,⁴⁵ A. Filipčić,^{66,52} I. Fleck,¹⁹ S. Fliescher,⁶⁰ C.E. Fracchiolla,²⁶ E.D. Fraenkel,⁵⁸ U. Fröhlich,¹⁹ W. Fulgione,³ R.F. Gamarra,⁴⁵ S. Gambetta,⁶⁷ B. García,¹ D. García Gámez,⁴⁰ D. Garcia-Pinto,¹³ X. Garrido,^{16,49} G. Gelmini,¹⁴ H. Gemmeke,²¹ P.L. Ghia,^{59,3} U. Giaccari,³³ M. Giller,⁶⁸ H. Glass,⁴ L.M. Goggin,¹⁰ M.S. Gold,²⁷ G. Golup,⁶ F. Gomez Albarracin,²⁰ M. Gómez Berisso,⁶ P. Gonçalves,² D. Gonzalez,³⁴ J.G. Gonzalez,^{40,69} D. Góra,^{34,37} A. Gorgi,³ P. Gouffon,⁷⁰ S.R. Gozzini,³⁹ E. Grashorn,²⁵ S. Grebe,⁴⁷ M. Grigat,⁶⁰ A.F. Grillo,⁷¹ Y. Guardincerri,⁷² F. Guarino,⁹ G.P. Guedes,⁷³ J.D. Hague,²⁷ V. Halenka,⁷⁴ P. Hansen,²⁰ D. Harari,⁶ S. Harmsma,^{58,48} J.L. Harton,²⁶ A. Haungs,¹⁶ T. Hebbeker,⁶⁰ D. Heck,¹⁶ A.E. Herve,²² C. Hojvat,⁴ V.C. Holmes,²² P. Homola,³⁷ J.R. Hörandel,⁴⁷ A. Horneffer,⁴⁷ M. Hrabovský,^{74,35} T. Huege,¹⁶ M. Hussain,⁵² M. Iarlori,⁷⁵ A. Insolia,⁴² F. Ionita,¹⁷ A. Italiano,⁴² S. Jiraskova,⁴⁷ K. Kadija,¹¹ M. Kaducak,⁴ K.H. Kampert,²⁸ T. Karova,³⁵ P. Kasper,⁴ B. Kégl,⁴⁹ B. Keilhauer,¹⁶ A. Keivani,⁶⁹ J. Kelley,⁴⁷ E. Kemp,⁴⁴ R.M. Kieckhafer,⁶¹ H.O. Klages,¹⁶ M. Kleifges,²¹ J. Kleinfeller,¹⁶ R. Knapik,²⁶ J. Knapp,³⁹ D.-H. Koang,²⁹ A. Krieger,⁴⁵ O. Krömer,²¹ D. Kruppke-Hansen,²⁸ F. Kuehn,⁴ D. Kuempel,²⁸ K. Kulbartz,⁷⁶ N. Kunka,²¹ A. Kusenko,¹⁴ G. La Rosa,¹² C. Lachaud,⁵ B.L. Lago,⁵⁶ P. Lautridou,⁵³ M.S.A.B. Leão,⁷⁷ D. Lebrun,²⁹ P. Lebrun,⁴ J. Lee,¹⁴ M.A. Leigui de Oliveira,⁷⁷ A. Lemiére,⁵⁹ A. Letessier-Selvon,¹⁵ I. Lhenry-Yvon,⁵⁹ R. López,⁷⁸ A. Lopez Agüera,⁸ K. Louedec,⁴⁹ J. Lozano Bahilo,⁴⁰ A. Lucero,³ M. Ludwig,³⁴ H. Lyberis,⁵⁹ M.C. Maccarone,¹² C. Macolino,^{15,75} S. Maldera,³ D. Mandat,³⁵ P. Mantsch,⁴ A.G. Mariazzi,²⁰ V. Marin,⁵³ I.C. Maris,^{15,34} H.R. Marquez Falcon,⁵⁰ G. Marsella,⁷⁹ D. Martello,³³ O. Martínez Bravo,⁷⁸ H.J. Mathes,¹⁶ J. Matthews,^{69,80} J.A.J. Matthews,²⁷ G. Matthiae,³⁶ D. Maurizio,⁴³ P.O. Mazur,⁴ M. McEwen,³² G. Medina-Tanco,⁵⁴ M. Melissas,³⁴ D. Melo,⁴³ E. Menichetti,⁴³ A. Menshikov,²¹ C. Meurer,⁶⁰ S. Mićanović,¹¹ M.I. Micheletti,⁴⁵ W. Miller,²⁷ L. Miramonti,⁵⁵ S. Mollerach,⁶ M. Monasor,^{17,13} D. Monnier Ragaigne,⁴⁹ F. Montanet,²⁹ B. Morales,⁵⁴ C. Morello,³ E. Moreno,⁷⁸ J.C. Moreno,²⁰ C. Morris,²⁵ M. Mostafá,²⁶ S. Mueller,¹⁶ M.A. Muller,⁴⁴ R. Mussa,⁴³ G. Navarra,^{3,*} J.L. Navarro,⁴⁰ S. Navas,⁴⁰ P. Necosal,³⁵ L. Nellen,⁵⁴ P.T. Nhung,⁶³ N. Nierstenhoefer,²⁸ D. Nitz,⁶¹ D. Nosek,⁸¹ L. Nožka,³⁵ M. Nyklicek,³⁵ J. Oehlschläger,¹⁶ A. Olinto,¹⁷ P. Oliva,²⁸ V.M. Olmos-Gilbaja,⁸ M. Ortiz,¹³ N. Pacheco,³² D. Pakk Selmi-Dei,⁴⁴ M. Palatka,³⁵ J. Pallotta,⁸² N. Palmieri,³⁴ G. Parente,⁸ E. Parizot,⁵ S. Parlati,⁷¹ A. Parra,⁸ J. Parrisius,³⁴ R.D. Parsons,³⁹ S. Pastor,⁸³ T. Paul,⁸⁴ V. Pavlidou,^{17,85} K. Payet,²⁹ M. Pech,³⁵ J. Pękala,³⁷ R. Pelayo,⁸ I.M. Pepe,⁸⁶ L. Perrone,⁷⁹ R. Pesce,⁶⁷ E. Petermann,⁸⁷ S. Petrera,^{75,88} P. Petrinca,³⁶ A. Petrolini,⁶⁷ Y. Petrov,²⁶ J. Petrovic,⁴⁸ C. Pfendner,³⁰ R. Piegaiia,⁷² T. Pierog,¹⁶ M. Pimenta,² V. Pirronello,⁴² M. Platino,⁴⁵ V.H. Ponce,⁶ M. Pontz,¹⁹ P. Privitera,¹⁷ M. Prouza,³⁵ E.J. Quel,⁸² J. Rautenberg,²⁸ O. Ravel,⁵³ D. Ravignani,⁴⁵ A. Redondo,³² B. Revenu,⁵³ F.A.S. Rezende,²³ J. Ridky,³⁵ S. Riggi,⁴² M. Risse,^{19,28} P. Ristori,⁸² C. Rivière,²⁹ V. Rizi,⁷⁵ C. Robledo,⁷⁸ G. Rodriguez,^{8,36} J. Rodriguez

Martino,^{46,42} J. Rodriguez Rojo,⁴⁶ I. Rodriguez-Cabo,⁸ M.D. Rodríguez-Frías,³² G. Ros,³² J. Rosado,¹³ T. Rossler,⁷⁴ M. Roth,¹⁶ B. Rouillé-d’Orfeuil,^{17,5} E. Roulet,⁶ A.C. Rovero,⁸⁹ F. Salamida,^{16,75} H. Salazar,^{78,90} G. Salina,³⁶ F. Sánchez,^{45,54} M. Santander,⁴⁶ C.E. Santo,² E. Santos,² E.M. Santos,⁵⁶ F. Sarazin,⁹¹ S. Sarkar,⁹² R. Sato,⁴⁶ N. Scharf,⁶⁰ V. Scherini,²⁸ H. Schieler,¹⁶ P. Schiffer,⁶⁰ A. Schmidt,²¹ F. Schmidt,¹⁷ T. Schmidt,³⁴ O. Scholten,⁵⁸ H. Schoorlemmer,⁴⁷ J. Schovancova,³⁵ P. Schovánek,³⁵ F. Schroeder,¹⁶ S. Schulte,⁶⁰ F. Schüssler,¹⁶ D. Schuster,⁹¹ S.J. Sciutto,²⁰ M. Scuderi,⁴² A. Segreto,¹² D. Semikoz,⁵ M. Settimo,³³ R.C. Shellard,^{23,62} I. Sidelnik,⁴⁵ B.B. Siffert,⁵⁶ G. Sigl,⁷⁶ A. Śmiałkowski,⁶⁸ R. Šmída,^{16,35} G.R. Snow,⁸⁷ P. Sommers,⁵¹ J. Sorokin,²² H. Spinka,^{93,4} R. Squartini,⁴⁶ J. Stasielak,³⁷ M. Stephan,⁶⁰ E. Strazzeri,^{12,49} A. Stutz,²⁹ F. Suarez,⁴⁵ T. Suomijärvi,⁵⁹ A.D. Supanitsky,⁵⁴ T. Šuša,¹¹ M.S. Sutherland,²⁵ J. Swain,⁸⁴ Z. Szadkowski,^{28,68} A. Tamashiro,⁸⁹ A. Tamburro,³⁴ A. Tapia,⁴⁵ T. Tarutina,²⁰ O. Taşcau,²⁸ R. Tcaciuc,¹⁹ D. Tcherniakhovski,²¹ D. Tegolo,^{42,94} N.T. Thao,⁶³ D. Thomas,²⁶ J. Tiffenberg,⁷² C. Timmermans,^{48,47} W. Tkaczyk,⁶⁸ C.J. Todero Peixoto,⁷⁷ B. Tomé,² A. Tonachini,⁴³ P. Travnicek,³⁵ D.B. Tridapalli,⁷⁰ G. Tristram,⁵ E. Trovato,⁴² M. Tueros,²⁰ R. Ulrich,^{51,16} M. Unger,¹⁶ M. Urban,⁴⁹ J.F. Valdés Galicia,⁵⁴ I. Valiño,¹⁶ L. Valore,⁹ A.M. van den Berg,⁵⁸ J.R. Vázquez,¹³ R.A. Vázquez,⁸ D. Veberič,^{52,66} T. Venters,¹⁷ V. Verzi,³⁶ M. Videla,¹ L. Villaseñor,⁵⁰ S. Vorobiov,⁵² L. Voyvodic,^{4,*} H. Wahlberg,²⁰ P. Wahrlich,²² O. Wainberg,⁴⁵ D. Warner,²⁶ A.A. Watson,³⁹ S. Westerhoff,³⁰ B.J. Whelan,²² G. Wieczorek,⁶⁸ L. Wiencke,⁹¹ B. Wilczyńska,³⁷ H. Wilczyński,³⁷ C. Williams,¹⁷ T. Winchen,⁶⁰ M.G. Winnick,²² B. Wundheiler,⁴⁵ T. Yamamoto,^{17,95} P. Younk,²⁶ G. Yuan,⁶⁹ A. Yushkov,⁹ E. Zas,⁸ D. Zavrtanik,^{52,66} M. Zavrtanik,^{66,52} I. Zaw,⁷ A. Zepeda,⁹⁶ and M. Ziolkowski¹⁹

¹National Technological University, Faculty Mendoza (CONICET/CNEA), Mendoza, Argentina

²LIP and Instituto Superior Técnico, Lisboa, Portugal

³Istituto di Fisica dello Spazio Interplanetario (INAF),
Università di Torino and Sezione INFN, Torino, Italy

⁴Fermilab, Batavia, IL, USA

⁵Laboratoire AstroParticule et Cosmologie (APC),
Université Paris 7, CNRS-IN2P3, Paris, France

⁶Centro Atómico Bariloche and Instituto Balseiro (CNEA-UNCuyo-CONICET), San Carlos de Bariloche, Argentina

⁷New York University, New York, NY, USA

⁸Universidad de Santiago de Compostela, Spain

⁹Università di Napoli “Federico II” and Sezione INFN, Napoli, Italy

¹⁰University of Wisconsin, Milwaukee, WI, USA

¹¹Rudjer Bošković Institute, 10000 Zagreb, Croatia

¹²Istituto di Astrofisica Spaziale e Fisica Cosmica di Palermo (INAF), Palermo, Italy

¹³Universidad Complutense de Madrid, Madrid, Spain

¹⁴University of California, Los Angeles, CA, USA

¹⁵Laboratoire de Physique Nucléaire et de Hautes Energies (LPNHE),
Universités Paris 6 et Paris 7, CNRS-IN2P3, Paris, France

¹⁶Karlsruhe Institute of Technology - Campus North - Institut für Kernphysik, Karlsruhe, Germany

¹⁷University of Chicago, Enrico Fermi Institute, Chicago, IL, USA

¹⁸Pierre Auger Southern Observatory and Comisión Nacional de Energía Atómica, Malargüe, Argentina

¹⁹Universität Siegen, Siegen, Germany

²⁰IFLP, Universidad Nacional de La Plata and CONICET, La Plata, Argentina

²¹Karlsruhe Institute of Technology - Campus North - Institut für Prozessdatenverarbeitung und Elektronik, Karlsruhe, Germany

²²University of Adelaide, Adelaide, S.A., Australia

²³Centro Brasileiro de Pesquisas Físicas, Rio de Janeiro, RJ, Brazil

²⁴Universidade Estadual do Sudoeste da Bahia, Vitória da Conquista, BA, Brazil

²⁵Ohio State University, Columbus, OH, USA

²⁶Colorado State University, Fort Collins, CO, USA

²⁷University of New Mexico, Albuquerque, NM, USA

²⁸Bergische Universität Wuppertal, Wuppertal, Germany

²⁹Laboratoire de Physique Subatomique et de Cosmologie (LPSC),
Université Joseph Fourier, INPG, CNRS-IN2P3, Grenoble, France

³⁰University of Wisconsin, Madison, WI, USA

³¹Max-Planck-Institut für Radioastronomie, Bonn, Germany

³²Universidad de Alcalá, Alcalá de Henares (Madrid), Spain

³³Dipartimento di Fisica dell’Università del Salento and Sezione INFN, Lecce, Italy

³⁴Karlsruhe Institute of Technology - Campus South - Institut für Experimentelle Kernphysik (IEKP), Karlsruhe, Germany

³⁵Institute of Physics of the Academy of Sciences of the Czech Republic, Prague, Czech Republic

³⁶Università di Roma II “Tor Vergata” and Sezione INFN, Roma, Italy

³⁷Institute of Nuclear Physics PAN, Krakow, Poland

- ³⁸Colorado State University, Pueblo, CO, USA
- ³⁹School of Physics and Astronomy, University of Leeds, United Kingdom
- ⁴⁰Universidad de Granada & C.A.F.P.E., Granada, Spain
- ⁴¹Case Western Reserve University, Cleveland, OH, USA
- ⁴²Università di Catania and Sezione INFN, Catania, Italy
- ⁴³Università di Torino and Sezione INFN, Torino, Italy
- ⁴⁴Universidade Estadual de Campinas, IFGW, Campinas, SP, Brazil
- ⁴⁵Centro Atómico Constituyentes (Comisión Nacional de Energía Atómica/CONICET/UTN-FRBA), Buenos Aires, Argentina
- ⁴⁶Pierre Auger Southern Observatory, Malargüe, Argentina
- ⁴⁷IMAPP, Radboud University, Nijmegen, Netherlands
- ⁴⁸NIKHEF, Amsterdam, Netherlands
- ⁴⁹Laboratoire de l'Accélérateur Linéaire (LAL), Université Paris 11, CNRS-IN2P3, Orsay, France
- ⁵⁰Universidad Michoacana de San Nicolas de Hidalgo, Morelia, Michoacan, Mexico
- ⁵¹Pennsylvania State University, University Park, PA, USA
- ⁵²Laboratory for Astroparticle Physics, University of Nova Gorica, Slovenia
- ⁵³SUBATECH, CNRS-IN2P3, Nantes, France
- ⁵⁴Universidad Nacional Autonoma de Mexico, Mexico, D.F., Mexico
- ⁵⁵Università di Milano and Sezione INFN, Milan, Italy
- ⁵⁶Universidade Federal do Rio de Janeiro, Instituto de Física, Rio de Janeiro, RJ, Brazil
- ⁵⁷Universidade de São Paulo, Instituto de Física, São Carlos, SP, Brazil
- ⁵⁸Kernfysisch Versneller Instituut, University of Groningen, Groningen, Netherlands
- ⁵⁹Institut de Physique Nucléaire d'Orsay (IPNO), Université Paris 11, CNRS-IN2P3, Orsay, France
- ⁶⁰RWTH Aachen University, III. Physikalisches Institut A, Aachen, Germany
- ⁶¹Michigan Technological University, Houghton, MI, USA
- ⁶²Pontificia Universidade Católica, Rio de Janeiro, RJ, Brazil
- ⁶³Institute for Nuclear Science and Technology (INST), Hanoi, Vietnam
- ⁶⁴University of Hawaii, Honolulu, HI, USA
- ⁶⁵ASTRON, Dwingeloo, Netherlands
- ⁶⁶J. Stefan Institute, Ljubljana, Slovenia
- ⁶⁷Dipartimento di Fisica dell'Università and INFN, Genova, Italy
- ⁶⁸University of Łódź, Łódź, Poland
- ⁶⁹Louisiana State University, Baton Rouge, LA, USA
- ⁷⁰Universidade de São Paulo, Instituto de Física, São Paulo, SP, Brazil
- ⁷¹INFN, Laboratori Nazionali del Gran Sasso, Assergi (L'Aquila), Italy
- ⁷²Departamento de Física, FCEyN, Universidad de Buenos Aires y CONICET, Argentina
- ⁷³Universidade Estadual de Feira de Santana, Brazil
- ⁷⁴Palacký University, Olomouc, Czech Republic
- ⁷⁵Università dell'Aquila and INFN, L'Aquila, Italy
- ⁷⁶Universität Hamburg, Hamburg, Germany
- ⁷⁷Universidade Federal do ABC, Santo André, SP, Brazil
- ⁷⁸Benemérita Universidad Autónoma de Puebla, Puebla, Mexico
- ⁷⁹Dipartimento di Ingegneria dell'Innovazione dell'Università del Salento and Sezione INFN, Lecce, Italy
- ⁸⁰Southern University, Baton Rouge, LA, USA
- ⁸¹Charles University, Faculty of Mathematics and Physics, Institute of Particle and Nuclear Physics, Prague, Czech Republic
- ⁸²Centro de Investigaciones en Láseres y Aplicaciones, CITEFA and CONICET, Argentina
- ⁸³Instituto de Física Corpuscular, CSIC-Universitat de València, Valencia, Spain
- ⁸⁴Northeastern University, Boston, MA, USA
- ⁸⁵Caltech, Pasadena, USA
- ⁸⁶Universidade Federal da Bahia, Salvador, BA, Brazil
- ⁸⁷University of Nebraska, Lincoln, NE, USA
- ⁸⁸Gran Sasso Center for Astroparticle Physics, Italy
- ⁸⁹Instituto de Astronomía y Física del Espacio (CONICET), Buenos Aires, Argentina
- ⁹⁰Instituto Nacional de Astrofísica, Óptica y Electrónica, Puebla, Mexico
- ⁹¹Colorado School of Mines, Golden, CO, USA
- ⁹²Rudolf Peierls Centre for Theoretical Physics, University of Oxford, Oxford, United Kingdom
- ⁹³Argonne National Laboratory, Argonne, IL, USA
- ⁹⁴Università di Palermo and Sezione INFN, Catania, Italy
- ⁹⁵Konan University, Kobe, Japan
- ⁹⁶Centro de Investigación y de Estudios Avanzados del IPN (CINVESTAV), México, D.F., Mexico

(Dated: August 20, 2018)

We describe the measurement of the depth of maximum, X_{\max} , of the longitudinal development of air showers induced by cosmic rays. Almost four thousand events above 10^{18} eV observed by the fluorescence detector of the Pierre Auger Observatory in coincidence with at least one surface detector station are selected for the analysis. The average shower maximum was found to evolve with energy at a rate of (106_{-21}^{+35}) g/cm²/decade below $10^{18.24 \pm 0.05}$ eV and (24 ± 3) g/cm²/decade above this energy. The measured shower-to-shower fluctuations decrease from about 55 to 26 g/cm². The interpretation of these results in terms of the cosmic ray mass composition is briefly discussed.

PACS numbers: 96.50.sd,13.85.Tp,98.70.Sa

Introduction – The energy dependence of the mass composition of cosmic rays is, along with the flux and arrival direction distribution, an important parameter for the understanding of the sources and propagation of cosmic rays at very high energy. There are several models that describe the observed flux of cosmic rays very well, but each of these models has different assumptions about the cosmic ray sources and correspondingly predicts a different mass composition at Earth. For example, the hardening of the cosmic ray energy spectrum at energies between 10^{18} eV and 10^{19} eV, known as the ‘ankle’, is presumed to be either a signature of the transition from galactic to extragalactic cosmic rays or a distortion of a proton-dominated extragalactic spectrum due to energy losses [1]. Moreover, composition information may eventually help to decide whether the flux suppression observed above $4 \cdot 10^{19}$ eV [2] is due mainly to the interaction of cosmic rays with the microwave background or a signature of the maximum injection energy of the sources [3].

Due to the low flux at these energies, the composition of cosmic rays cannot be measured directly, but has to be inferred from observations of extensive air showers. The atmospheric depth, X_{\max} , at which the longitudinal development of a shower reaches its maximum in terms of the number of secondary particles is correlated with the mass of the incident cosmic ray particle. With the generalization of Heitler’s model of electron-photon cascades to hadron-induced showers and the superposition assumption for nuclear primaries of mass A , the average depth of the shower maximum, $\langle X_{\max} \rangle$, at a given energy E is expected to follow [4]

$$\langle X_{\max} \rangle = \alpha (\ln E - \langle \ln A \rangle) + \beta, \quad (1)$$

where $\langle \ln A \rangle$ is the average of the logarithm of the primary masses. The coefficients α and β depend on the nature of hadronic interactions, most notably on the multiplicity, elasticity and cross-section in ultra-high energy collisions of hadrons with air, see e.g. [5]. Although Eq. (1) is based on a simplified description of air showers, it gives a good description of air shower simulations with energy-independent parameters α and β in the energy range considered here, see [6]. Only physics processes not accounted for in currently available interaction models could lead to a significant energy dependence of these parameters.

The change of $\langle X_{\max} \rangle$ per decade of energy is called *elongation rate* [7],

$$D_{10} = \frac{d\langle X_{\max} \rangle}{d \lg E} \approx \alpha \left(1 - \frac{d\langle \ln A \rangle}{d \ln E} \right) \ln(10), \quad (2)$$

and it is sensitive to changes in composition with energy. A complementary composition-dependent observable is the magnitude of the shower-to-shower fluctuations of the depth of maximum, $\text{RMS}(X_{\max})$, which is expected to decrease with the number of primary nucleons A (though not as fast as $1/\sqrt{A}$ [8]) and to increase with the interaction length of the primary particle.

At ultra high energies, the shower maximum can be observed directly with fluorescence detectors. Previously published X_{\max} measurements [9, 10] focused mainly on $\langle X_{\max} \rangle$ as a function of energy and had only limited statistics above 10^{19} eV.

Here we present a measurement of both $\langle X_{\max} \rangle$ and $\text{RMS}(X_{\max})$ using high quality and high statistics data collected with the southern site of the Pierre Auger Observatory [11]. The Observatory is located in the province of Mendoza, Argentina and consists of two detectors. The surface detector (SD) array comprises 1600 water-Cherenkov detectors arranged on a triangular grid with 1500 m spacing that cover an area of over 3000 km². The water-Cherenkov detectors are sensitive to the air shower components at ground level. The fluorescence detector (FD) consists of 24 optical telescopes overlooking the array, which can observe the longitudinal shower development by detecting the fluorescence and Cherenkov light produced by charged particles along the shower trajectory in the atmosphere.

Data Analysis. – This work is based on air shower data recorded between December 2004 and March 2009. Only events detected in hybrid mode [12] are considered, i.e. the shower development must have been measured by the FD, and at least one coincident SD station is required to provide a ground-level time. Using the time constraint from the SD, the shower geometry can be determined with an angular uncertainty of 0.6° [13]. The longitudinal profile of the energy deposit is reconstructed [14] from the light recorded by the FD using the fluorescence and Cherenkov yields and lateral distributions from [15]. With the help of data from atmospheric monitoring devices [16] the light collected by the telescopes is corrected for the attenuation between the shower and the detector

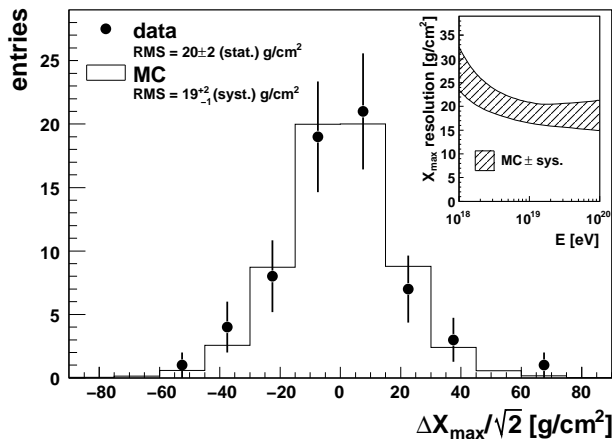


FIG. 1: Difference between X_{\max} measured in showers simultaneously at two FD stations ($\langle \lg(E/\text{eV}) \rangle = 19.1$). The X_{\max} resolution is displayed as a function of energy in the inset.

and the longitudinal shower profile is reconstructed as a function of atmospheric depth. X_{\max} is determined by fitting the reconstructed longitudinal profile with a Gaisser-Hillas function [17].

An unbiased set of high quality events is selected with the statistical uncertainty of the reconstructed X_{\max} being comparable to the size of the fluctuations expected for nuclei as heavy as iron ($\approx 20 \text{ g/cm}^2$) and small systematic uncertainties as explained in the following.

The impact of varying atmospheric conditions on the X_{\max} measurement is minimized by rejecting time periods with cloud coverage and by requiring reliable measurements of the vertical optical depth of aerosols. Profiles that are distorted by residual cloud contamination are rejected by a loose cut on the quality of the profile fit ($\chi^2/\text{Ndf} < 2.5$). We take into account events only with energies above 10^{18} eV where the probability for at least one triggered SD station is 100%, irrespective of the mass of the primary particle [18]. The geometrical reconstruction of showers with a large apparent angular speed of the image in the telescope is susceptible to uncertainties in the time synchronization between FD and SD. Therefore, events with a light emission angle towards the FD that is smaller than 20° are rejected. This cut also removes events with a large fraction of Cherenkov light. The energy and shower maximum can be reliably measured only if X_{\max} is in the field of view (FOV) of the telescopes (covering 1.5° to 30° in elevation). Events for which only the rising or falling edge of the profile is detected are not used. Moreover, we calculate the expected statistical uncertainty of the reconstruction of X_{\max} for each event, based on the shower geometry and atmospheric conditions, and require it to be better than 40 g/cm^2 .

The latter two selection criteria may cause a selection bias due to a systematic undersampling of the tails of the true X_{\max} distribution, since showers developing very

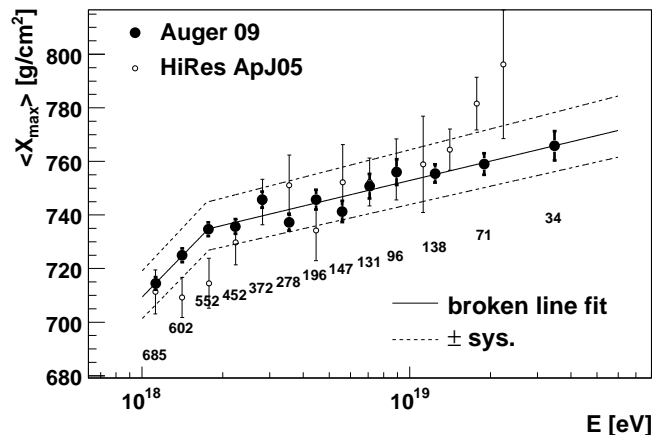


FIG. 2: $\langle X_{\max} \rangle$ as a function of energy. Lines denote a fit with a broken line in $\lg E$. The systematic uncertainties of $\langle X_{\max} \rangle$ are indicated by a dashed line. The number of events in each energy bin is displayed below the data points. HiRes data [10] are shown for comparison.

deep or shallow in the atmosphere might be rejected from the data sample. To avoid such a bias in the measured $\langle X_{\max} \rangle$ and $\text{RMS}(X_{\max})$ we apply fiducial volume cuts based on the shower geometry that ensure that the viewable X_{\max} range for each shower is large enough to accommodate the full X_{\max} distribution [19].

After all cuts, 3754 events are selected for the X_{\max} analysis. The X_{\max} resolution as a function of energy for these events is estimated using a detailed simulation of the FD and the atmosphere. As shown in the inset of Fig. 1, the resolution is at the 20 g/cm^2 level above a few EeV. The difference between the reconstructed X_{\max} values in events that had a sufficiently high energy to be detected independently by two or more FD stations is used to cross-check these findings. As can be seen in Fig. 1, the simulations reproduce the data well.

Results and Discussion. – The measured $\langle X_{\max} \rangle$ and $\text{RMS}(X_{\max})$ values are shown in Figs. 2 and 3. We use bins of $\Delta \lg E = 0.1$ below 10 EeV and $\Delta \lg E = 0.2$ above that energy. The last bin starts at $10^{19.4} \text{ eV}$, integrating up to the highest energy event ($E = (59 \pm 8) \text{ EeV}$). The systematic uncertainty of the FD energy scale is 22% [18]. Uncertainties of the calibration, atmospheric conditions, reconstruction and event selection give rise to a systematic uncertainty of $\leq 13 \text{ g/cm}^2$ for $\langle X_{\max} \rangle$ and $\leq 6 \text{ g/cm}^2$ for the RMS. The results were found to be independent of zenith angle, time periods and FD stations within the experimental uncertainties.

A fit of the measured $\langle X_{\max} \rangle$ values with a constant elongation rate does not describe our data ($\chi^2/\text{Ndf} = 34.9/11$), but as can be seen in Fig. 2, using two slopes yields a satisfactory fit ($\chi^2/\text{Ndf} = 9.7/9$) with an elongation rate of $(106_{-21}^{+35}) \text{ g/cm}^2/\text{decade}$ below $10^{18.24 \pm 0.05} \text{ eV}$ and $(24 \pm 3) \text{ g/cm}^2/\text{decade}$ above this en-

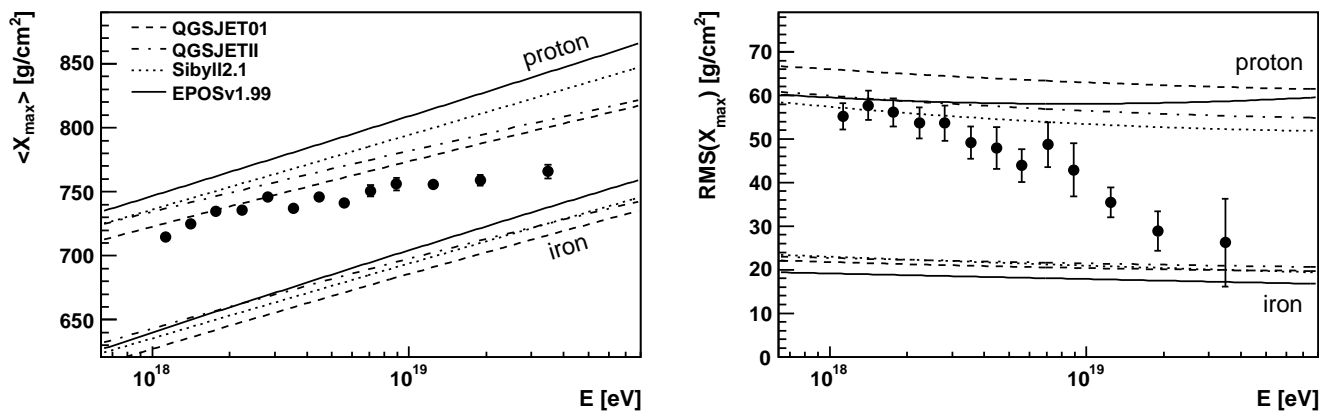


FIG. 3: $\langle X_{\max} \rangle$ and $RMS(X_{\max})$ compared with air shower simulations [20] using different hadronic interaction models[21].

ergy. If the properties of hadronic interactions do not change significantly over less than two orders of magnitude in primary energy ($<$ factor 10 in center of mass energy), this change of $\Delta D_{10} = (82^{+35}_{-21}) g/cm^2/decade$ would imply a change in the energy dependence of the composition around the ankle, supporting the hypothesis of a transition from galactic to extragalactic cosmic rays in this region.

The $\langle X_{\max} \rangle$ result of this analysis is compared to the HiRes data [10] in Fig. 2. Both data-sets agree well within the quoted systematic uncertainties. The χ^2/Ndf of the HiRes data with respect to the broken-line fit described above is 20.5/14. This value reduces to 16.8/14 if a relative energy shift of 15% is applied, such as suggested by a comparison of the Auger and HiRes energy spectra [2].

The shower-to-shower fluctuations, $RMS(X_{\max})$, are obtained by subtracting the detector resolution in quadrature from the width of the observed X_{\max} distributions resulting in a correction of $\leq 6 g/cm^2$. As can be seen in the right panel of Fig. 3, we observe a decrease in the fluctuations with energy from about 55 to 26 g/cm^2 as the energy increases. Assuming again that the hadronic interaction properties do not change much within the observed energy range, these decreasing fluctuations are an independent signature of an increasing average mass of the primary particles.

For the interpretation of the absolute values of $\langle X_{\max} \rangle$ and $RMS(X_{\max})$ a comparison to air shower simulations is needed. As can be seen in Fig. 3, there are considerable differences between the results of calculations using different hadronic interaction models. These differences are not necessarily exhaustive, since the hadronic interaction models do not cover the full range of possible extrapolations of low energy accelerator data. If, however, these models provide a realistic description of hadronic interactions at ultra high energies, the comparison of the data and simulations leads to the same conclusions as above,

namely a gradual increase of the average mass of cosmic rays with energy up to 59 EeV.

Acknowledgments. – The successful installation and commissioning of the Pierre Auger Observatory would not have been possible without the strong commitment and effort from the technical and administrative staff in Malargüe. We are very grateful to the following agencies and organizations for financial support: Comisión Nacional de Energía Atómica, Fundación Antorchas, Gobierno De La Provincia de Mendoza, Municipalidad de Malargüe, NDM Holdings and Valle Las Leñas, in gratitude for their continuing cooperation over land access, Argentina; the Australian Research Council; Conselho Nacional de Desenvolvimento Científico e Tecnológico (CNPq), Financiadora de Estudos e Projetos (FINEP), Fundação de Amparo à Pesquisa do Estado de Rio de Janeiro (FAPERJ), Fundação de Amparo à Pesquisa do Estado de São Paulo (FAPESP), Ministério de Ciência e Tecnologia (MCT), Brazil; AVCR AV0Z10100502 and AV0Z10100522, GAAV KJB300100801 and KJB100100904, MSMT-CR LA08016, LC527, 1M06002, and MSM0021620859, Czech Republic; Centre de Calcul IN2P3/CNRS, Centre National de la Recherche Scientifique (CNRS), Conseil Régional Ile-de-France, Département Physique Nucléaire et Corpusculaire (PNC-IN2P3/CNRS), Département Sciences de l’Univers (SDU-INSU/CNRS), France; Bundesministerium für Bildung und Forschung (BMBF), Deutsche Forschungsgemeinschaft (DFG), Finanzministerium Baden-Württemberg, Helmholtz-Gemeinschaft Deutscher Forschungszentren (HGF), Ministerium für Wissenschaft und Forschung, Nordrhein-Westfalen, Ministerium für Wissenschaft, Forschung und Kunst, Baden-Württemberg, Germany; Istituto Nazionale di Fisica Nucleare (INFN), Ministero dell’Istruzione, dell’Università e della Ricerca (MIUR), Italy; Consejo Nacional de Ciencia y Tecnología (CONACYT), Mexico; Ministerie van Onderwijs, Cultuur en Wetenschap, Nederlandse Organ-

isatie voor Wetenschappelijk Onderzoek (NWO), Stichting voor Fundamenteel Onderzoek der Materie (FOM), Netherlands; Ministry of Science and Higher Education, Grant Nos. 1 P03 D 014 30, N202 090 31/0623, and PAP/218/2006, Poland; Fundação para a Ciência e a Tecnologia, Portugal; Ministry for Higher Education, Science, and Technology, Slovenian Research Agency, Slovenia; Comunidad de Madrid, Consejería de Educación de la Comunidad de Castilla La Mancha, FEDER funds, Ministerio de Ciencia e Innovación, Xunta de Galicia, Spain; Science and Technology Facilities Council, United Kingdom; Department of Energy, Contract Nos. DE-AC02-07CH11359, DE-FR02-04ER41300, National Science Foundation, Grant No. 0450696, The Grainger Foundation USA; ALFA-EC / HELEN, European Union 6th Framework Program, Grant No. MEIF-CT-2005-025057, European Union 7th Framework Program, Grant No. PIEF-GA-2008-220240, and UNESCO.

* Deceased

- [1] A.M. Hillas, Phys. Lett. **24**, 677; V.S. Berezhinsky and S.I. Grigor'eva, Astron. Astrophys. **199** (1988), 1; D. Allard, E. Parizot and A. V. Olinto, Astropart. Phys. **27** (2007), 61; R. Aloisio, V. Berezhinsky, P. Blasi and S. Ostapchenko, Phys. Rev. D **77** (2008), 025007.
- [2] R. Abbasi *et al.* [HiRes Coll.], Phys. Rev. Lett. **100** (2008), 101101; J. Abraham *et al.* [Pierre Auger Coll.], Phys. Rev. Lett. **101** (2008), 061101.
- [3] D. Allard *et al.*, JCAP **0810** (2008), 033.
- [4] W. Heitler, Oxford University Press, 1954; J. Matthews, Astropart. Phys. **22** (2005), 387.
- [5] T. Wibig, Phys. Rev. D **79** (2009), 094008; R. Ulrich *et al.*, Proc. 31st ICRC (2009), arXiv:0906.0418.
- [6] T. Pierog, R. Engel and D. Heck, Czech. J. Phys. **56** (2006) A161; J. Bluemer, R. Engel and J. R. Hoerandel, Prog. Part. Nucl. Phys. **63**, 293 (2009) arXiv:0904.0725.
- [7] J. Linsley, Proc. 15th ICRC **12** (1977), 89; T.K. Gaisser *et al.*, Proc. 16th ICRC **9** (1979), 258; J. Linsley and A.A. Watson, Phys. Rev. Lett. **46** (1981), 459.
- [8] J. Engel *et al.*, Phys. Rev. **D46** (1992), 5013.
- [9] D.J. Bird *et al.* [Fly's Eye Coll.], Phys. Rev. Lett. **71** (1993), 3401.
- [10] R. U. Abbasi *et al.* [HiRes Coll.], Astrophys. J. **622** (2005), 910.
- [11] J. Abraham *et al.* [Pierre Auger Coll.], Nucl. Instrum. Meth. **A523** (2004), 50; J. Abraham *et al.* [Pierre Auger Coll.], submitted to Nucl. Instr. Meth., arXiv:0907.4282; I. Allekotte *et al.* [Pierre Auger Coll.], Nucl. Instrum. Meth. A **586** (2008), 409.
- [12] P. Sommers, Astropart. Phys. **3** (1995), 349; B.R. Dawson *et al.*, Astropart. Phys. **5** (1996), 239.
- [13] C. Bonifazi *et al.* [Pierre Auger Coll.], Nucl. Phys. Proc. Suppl. **190** (2009) 20, arXiv:0901.3138.
- [14] M. Unger *et al.*, Nucl. Instrum. Meth. **A588** (2008), 433;
- [15] M.D. Roberts, J. Phys. G **31** (2005), 1291; D. Gora *et al.*, Astropart. Phys. **24** (2006), 484; F. Nerling *et al.*, Astropart. Phys. **24** (2006), 421; B.R. Dawson, M. Giller and G. Wieczorek, Proc. 30th ICRC (2007); B. Keilhauer *et al.*, Nucl. Instrum. Meth. **A597**, (2008), 99.
- [16] J. Abraham *et al.* [Pierre Auger Coll.], Proc. 31st ICRC (2009), arXiv:0906.2358.
- [17] T.K. Gaisser and A.M. Hillas, Proc. 15th ICRC, **8**, 353 (1977).
- [18] J. Abraham *et al.* [Pierre Auger Coll.], Proc. 31st ICRC (2009), arXiv:0906.2189.
- [19] M. Unger [Pierre Auger Coll.], Nucl. Phys. Proc. Suppl. **190** (2009), 240 [arXiv:0902.3787]; J.A. Bellido [Pierre Auger Coll.], Proc. XXth Rencontres de Blois (2008) [arXiv:0901.3389]
- [20] T. Bergmann *et al.*, Astropart. Phys. **26** (2007), 420.
- [21] N.N. Kalmykov and S.S. Ostapchenko, Phys. Atom. Nucl. **56** (1993), 346; S.S. Ostapchenko, Nucl. Phys. Proc. Suppl. **151** (2006), 143; T. Pierog and K. Werner, Phys. Rev. Lett. **101** (2008), 171101; E.J. Ahn *et al.*, Phys. Rev. **D80** (2009), 094003.